

## New CP violation measurements at LHC

Valeriia Lukashenko<sup>a,b,\*</sup> and Ramón Angel Ruiz Fernández<sup>c,†,\*</sup> on behalf of LHCb, ATLAS and CMS collaborations

<sup>a</sup>National Institute for Subatomic Physics (Nikhef),  
Science Park 105, 1098 XG, Amsterdam, the Netherlands

<sup>b</sup>Institute for Nuclear Research of the National Academy of Sciences (KINR)  
prospekt Nauky 47, 03680, Kyiv, Ukraine

<sup>c</sup>Instituto Galego de Física de Altas Enerxías (IGFAE),  
Universidade de Santiago de Compostela, 15782, Santiago de Compostela, Spain

E-mail: [valeriia.lukashenko@cern.ch](mailto:valeriia.lukashenko@cern.ch), [ramon.angel.ruiz.fernandez@cern.ch](mailto:ramon.angel.ruiz.fernandez@cern.ch)

In this proceeding, we present a summary of the latest CP-violation findings at LHC. We begin with an overview of  $\gamma$  measurements in  $B^\pm \rightarrow Dh^\pm$  decays with data collected in 2015-2018 by LHCb and the update on the  $\gamma$  combination from LHCb.

Next, an updated time-integrated CP asymmetry in  $D^0 \rightarrow K^+K^-$  decays with the 2015-2018 LHCb data sample is shown. In combination with the difference of time-integrated asymmetries from [1], direct CP-asymmetries in  $D^0 \rightarrow K^+K^-$  and  $D^0 \rightarrow \pi^+\pi^-$  decays are determined.

Additionally, we present the updated time-dependent CP-violation measurements of angles  $\beta$  from  $B^0 \rightarrow \psi K_S^0$  and  $\beta_s$  from  $B_s^0 \rightarrow J/\psi K^+K^-$  decays with 2015-2018 LHCb data sample. We also show the new measurement of CP-violating phase  $\phi_s^{s\bar{s}}$  in  $B_s^0 \rightarrow \phi\phi$  transitions with 2015-2018 LHCb data.

The new results are the world's best estimates of  $\beta$ ,  $\beta_s$  angles,  $\phi_s^{s\bar{s}}$  phase, CP-symmetry in  $D^0 \rightarrow K^+K^-$  and  $D^0 \rightarrow \pi^+\pi^-$  decays and the most precise determination of  $\gamma$  angle from a single experiment. Finally, we briefly outline the future prospects of CP-violation measurements at LHC.

21st Conference on flavour Physics and CP Violation (FPCP 2023)

29 May - 2 June 2023

Lyon, France

\*Speakers

†Speaker for "Measurement of  $B^0$  and  $B_s^0$  mixing phases at LHCb"

## 1. Introduction

Charge-Parity (CP) violation arises within the framework of the Standard Model (SM) as a consequence of an irreducible complex phase in the parametrization of the so-called Cabibbo-Kobayashi-Maskawa (CKM) matrix. The elements of this matrix characterize the strength of quark flavour transitions between the flavour eigenstates [2, 3]. Exploiting the unitary property of the CKM matrix, it is possible to define six triangles from the vanishing conditions in the complex plane. In this proceeding, we present the latest updates performed by the LHCb collaboration regarding three angles associated with these triangles, namely  $\gamma$ ,  $\beta$  and  $\beta_s$ , which are defined as [2, 3]:

$$\gamma = \arg\left(\frac{V_{ud}V_{ub}^*}{V_{cd}V_{cb}^*}\right), \quad \beta = \arg\left(-\frac{V_{cd}V_{cb}^*}{V_{td}V_{tb}^*}\right), \quad \beta_s = \arg\left(-\frac{V_{ts}V_{tb}^*}{V_{cs}V_{cb}^*}\right). \quad (1)$$

We also present the new results in the charm CP-violation sector, namely the measurement of time-integrated CP-asymmetry in  $D^0 \rightarrow K^+K^-$  decays from LHCb. We then discuss prospects for CP-violation measurements at LHC.

## 2. CKM angle $\gamma$ measurements

The CKM angle  $\gamma$  can be measured from clean tree-level processes in Standard Model. Theoretically,  $\gamma$  can be determined precisely ( $|\Delta\gamma| < 10^{-7}$ ) with a small irreducible error from the second-order electro-weak corrections [4]. This makes  $\gamma$  a strong tool for Standard Model tests, as tree-level transitions are not sensitive to New Physics contributions. The current experimental world average from [5] is compatible with the Standard Model prediction from [6].

Experimentally  $\gamma$  is measured via interference between Cabbibo-favoured (CF)  $b \rightarrow c$  transitions and Cabbibo-suppressed (CS)  $b \rightarrow u$  transitions. This can be observed in  $B^\pm \rightarrow Dh^\pm$  decays, where  $D$  is either  $D^0$  or  $\bar{D}^0$  and  $h^\pm = \pi^\pm, K^\pm$ .  $D$  mesons are reconstructed with final states  $f$  that are accessible for both  $D^0$  and  $\bar{D}^0$ . The  $B^\pm \rightarrow D(\rightarrow f)h^\pm$  is described with three phases: CP-violating  $\gamma$ , CP-conserving strong  $B$ -phase  $\delta_B$  difference and CP-conserving strong phase difference  $\delta_D$  in  $D$  decays, as illustrated in Fig. 1. The amplitude of a CF decay  $B \rightarrow D^0h^\pm$  is denoted as  $A$ . The amplitude of  $B \rightarrow D^0h^\pm$  is parametrized via a ratio  $r_B$  between a CS and a CF amplitude. The ratio of  $D^0$  to  $\bar{D}^0$  amplitudes to the final state  $f$  is denoted by  $r_D$ . For the doubly-Cabbibo suppressed decays of the  $D^0$ , this is given by  $\tan^4\theta_c \approx 0.05$ , while for CP final states its value is around 1.

The biggest uncertainty in measurements usually comes from the knowledge of the  $\delta_D$  strong phase. The value of  $\delta_D$  from the amplitude model is often unreliable, therefore if possible is taken from external measurements.

### 2.1 $\gamma$ from $B^\pm \rightarrow D[K^\mp\pi^\pm\pi^\pm\pi^\mp]h^\pm$ where $h^\pm = K^\pm, \pi^\pm$ with $9 \text{ fb}^{-1}$

LHCb released a new measurement of  $\gamma$  from  $B^\pm \rightarrow Dh^\pm$  decays with  $D \rightarrow K^\mp\pi^\pm\pi^\pm\pi^\mp$  [7]. The  $D \rightarrow K^\mp\pi^\pm\pi^\pm\pi^\mp$  decays are interesting because of the high branching fraction and only charged particles in the final state. Decays  $B^\pm \rightarrow D[K^\mp\pi^\pm\pi^\pm\pi^\mp]K^\pm(\pi^\pm)$  are suppressed and have more prominent interference effects, whereas  $B^\pm \rightarrow D[K^\pm\pi^\mp\pi^\pm\pi^\mp]K^\pm(\pi^\pm)$  are favoured and the interference is suppressed. The difference between the two decays is in the relative sign of the kaon

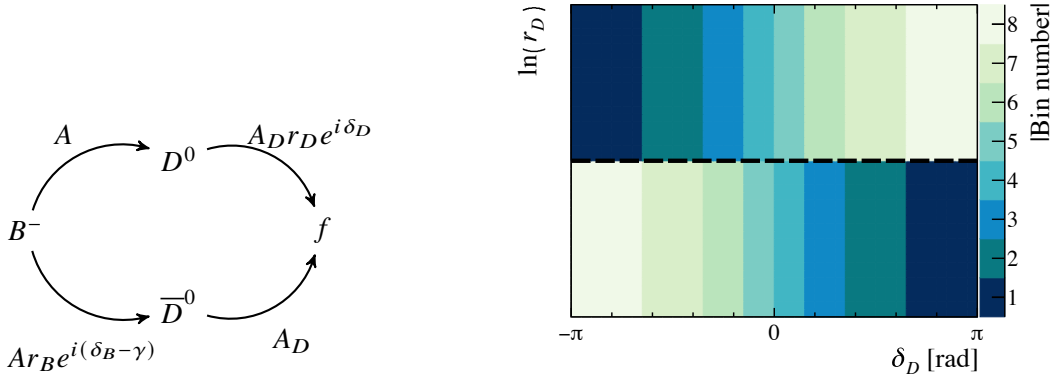


**Figure 1:** On the left the sketch of the amplitudes contributing to  $B^\pm \rightarrow Dh^\pm$  decays where  $D \rightarrow f$ .  $A$  and  $A_D$  are Cabibbo-favoured (CF) amplitudes of  $B$  and  $D$  decays, respectively;  $r_B$  and  $r_D$  are the ratio of Cabibbo-suppressed (CS) amplitude versus CF amplitude;  $\gamma$  is CP-violating phase difference;  $\delta_B$  and  $\delta_D$  are both CP-conserving phase differences. On the right is the binning scheme for the  $\gamma$  measurement from  $B^\pm \rightarrow D[K^+K^-\pi^+\pi^-]h^\pm$  and  $B^\pm \rightarrow D[\pi^+\pi^-\pi^+\pi^-]h^\pm$  decays.

from  $D$  decay with respect to the charged hadron from  $B$  decay. They are therefore referred to as “like-signed” (favoured) or “opposite-signed” (suppressed). To enhance sensitivity to  $\gamma$  further, phase space is binned in four bins of strong phase difference  $\delta_D$  [8]. The whole LHCb data with an integrated luminosity of  $9 \text{ fb}^{-1}$  is used.

The angle  $\gamma$  is determined from  $B$ -hadronic parameters: ratio of amplitudes  $r_B$  and strong-phase difference  $\delta_B$ . Both are defined in Fig. 1.  $D$ -hadronic parameters are taken from external results by CLEO-c [8], BESIII [9], LHCb [10].

Measured  $B$ -hadronic parameters from  $B^\pm \rightarrow DK^\pm$  and  $B^\pm \rightarrow D\pi^\pm$  decays are,

$$\begin{aligned} r_B^{DK} &= (94.6^{+3.1+0.5+3.0}_{-3.0-0.5-2.3}) \times 10^{-3}, \\ \delta_B^{DK} &= (134.6^{+6.0+0.7+8.6}_{-6.0-0.7-8.7})^\circ \\ r_B^{D\pi} &= (4.5^{+1.1+0.3+0.4}_{-1.0-0.3-0.3}) \times 10^{-3}, \\ \delta_B^{D\pi} &= (311.8^{+14.7+3.0+14.7}_{-15.0-2.3-15.0})^\circ. \end{aligned}$$

The first uncertainty is statistical, the second is systematic, and the last uncertainty is from the external inputs on  $D$ -hadronic parameters. The angle  $\gamma$  is determined to be

$$\gamma = (54.8^{+6.0+0.6+6.7}_{-5.8-0.6-4.2})^\circ,$$

and is consistent with the Standard Model expectation.

## 2.2 $\gamma$ from $B^\pm \rightarrow D[K^+K^-\pi^+\pi^-]h^\pm$ and $B^\pm \rightarrow D[\pi^+\pi^-\pi^+\pi^-]h^\pm$ with $9 \text{ fb}^{-1}$

Another measurement by LHCb exploits  $D \rightarrow K^+K^-\pi^+\pi^-$  and  $D \rightarrow \pi^+\pi^-\pi^+\pi^-$  decays [11]. The chosen binning scheme in the phase-space of  $D$  decays is two dimensional, in strong phase difference  $\delta_D$  and ratio of amplitudes  $r_D$ . In Fig. 1 binning scheme definition is shown on the right, where above the symmetry line, the  $D$ -meson decay is favoured and below is suppressed. A

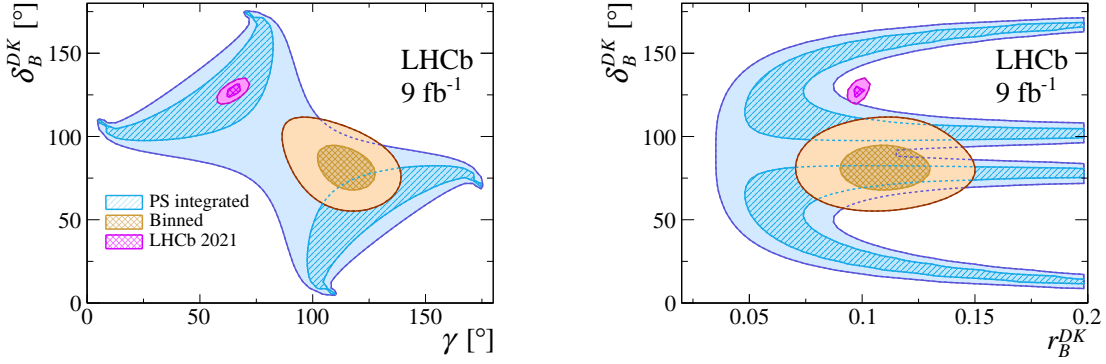


**Figure 2:** Two dimensional likelihood profiles for  $\gamma$ ,  $\delta_B$  and  $r_B$  from binned  $B^\pm \rightarrow D[K^+K^-\pi^+\pi^-]h^\pm$  measurement and phase-space integrated  $B^\pm \rightarrow D[\pi^+\pi^-\pi^+\pi^-]h^\pm$  measurement. The LHCb 2021 indicates the previous LHCb  $\gamma$  combination from [12].

phase-space integrated analysis is also performed with  $B^\pm \rightarrow D[\pi^+\pi^-\pi^+\pi^-]h^\pm$  decays.  $B$ -hadronic parameters with statistical and systematic uncertainties are measured to be

$$\begin{aligned} r_B^{DK} &= (110^{+20}_{-20}) \times 10^{-3}, \\ \delta_B^{DK} &= (81^{+14.0}_{-13.0})^\circ, \\ r_B^{D\pi} &= (4.1^{+5.4}_{-4.1}) \times 10^{-3}, \\ \delta_B^{D\pi} &= (298^{+62}_{-118})^\circ. \end{aligned}$$

In Fig. 2, the likelihood profiles are shown for both phase-space binned and integrated measurements. The binned measurement has better sensitivity and only one minimum, whereas the phase-space integrated measurement has two minima and worse sensitivity. The value of  $\gamma$  is found by the binned analysis to be,

$$\gamma = (116^{+12}_{-14})^\circ.$$

which is around 3 sigma from the LHCb average [12]. This result is model-dependent due to the absence of independent measurements on the  $D$ -hadronic parameters.

### 2.3 Updated LHCb $\gamma$ and $D^0 - \bar{D}^0$ mixing parameters combination

Combined measurement of  $\gamma$  and  $D^0 - \bar{D}^0$  mixing parameters based on the data collected by LHCb provides the most precise single experiment values for these parameters [12]. The combined measurement is updated with  $\gamma$  measurement with  $B^\pm \rightarrow D[K^\pm\pi^\mp\pi^\pm\pi^\mp]h^\pm$  decays [13],  $\gamma$  measurement with  $B^\pm \rightarrow D[h^+h^-\pi^0]h^\pm$  decays [14], mixing parameters  $y_{CP} - y_{CP}^{K\pi}$  measured using  $D^0 \rightarrow h^+h^-$  decays [15], measurement of time-integrated CP-asymmetry in  $D^0 \rightarrow K^+K^-$  decays [16], mixing parameters measured with  $D^0 \rightarrow K_s^0\pi^+\pi^-$  decays [17].

The new values for  $\gamma$  and  $D^0 - \bar{D}^0$  mixing parameters are [18]:

$$\begin{aligned} x_{CP} &= (0.389^{+0.050}_{-0.049}), \sigma\% \\ y_{CP} &= (0.636^{+0.020}_{-0.019}), \sigma\% \\ |q/p| &= 0.995^{+0.015}_{-0.016}, \\ \phi = \arg(q/p) &= 2.5 \pm 1.2^\circ, \\ \gamma &= (63.8^{+3.5}_{-3.7})^\circ. \end{aligned}$$

### 3. CP violation in charm

Standard Model CP violation in the charm sector is suppressed by the Cabbibo factor and GIM mechanism. The expected Standard Model CP asymmetry in charm is below 0.1%. Time-integrated CP asymmetry is defined as:

$$\mathcal{A}_{CP} = \frac{|A_f|^2 - |\bar{A}_f|^2}{|A_f|^2 + |\bar{A}_f|^2} \approx a_f^d + \frac{\langle t_D \rangle}{\tau_D} \Delta Y \quad (2)$$

where  $a_f^d$  is the direct CP-asymmetry;  $\langle t_D \rangle$  is the mean reconstructed decay time of  $D^0$ ;  $\tau_D$  is  $D^0$  lifetime and  $\Delta Y$  is the asymmetry between  $D^0 \rightarrow f$  and  $\bar{D}^0 \rightarrow f$  decay widths. LHCb has observed the first direct CP-asymmetry in  $D^0 \rightarrow h^+ h^-$  decays [1]. The difference between the direct CP asymmetries of  $D^0 \rightarrow K^+ K^-$  and  $D^0 \rightarrow \pi^+ \pi^-$  was measured to be non-zero with more than  $5\sigma$  significance. However, it is not clear whether the CP-asymmetry comes mainly from the  $D^0 \rightarrow K^+ K^-$  decays or  $D^0 \rightarrow \pi^+ \pi^-$  decay.

#### 3.1 CP asymmetry in $D^0 \rightarrow K^+ K^-$ decays

To understand the source of CP-asymmetry seen in [1], LHCb has measured the CP-asymmetry in  $D^0 \rightarrow K^+ K^-$  decays alone with  $5.7 \text{ fb}^{-1}$  of data [16]. To determine  $D^0$  mesons flavour, only  $D^0$  meson that originate from  $D^{*+} \rightarrow D^0 \pi^+$  were used. The additional  $\pi^+$  is used as a flavour tag for  $D^0$ . Experimentally  $\mathcal{A}_{CP}(K^+ K^-)$  from Eq. 2 is directly not accessible, and the so-called "raw" CP-asymmetry is measured as

$$A_{CP}^{raw} = \frac{N(D^{*+} \rightarrow D^0 \pi^+) - N(D^{*-} \rightarrow \bar{D}^0 \pi^-)}{N(D^{*+} \rightarrow D^0 \pi^+) + N(D^{*-} \rightarrow \bar{D}^0 \pi^-)} = \mathcal{A}_{CP}(K^+ K^-) + A_{det}(\pi_{tag}) + A_{prod}(D^{*+}), \quad (3)$$

where  $A_{det}$  is detector asymmetry of tag  $\pi$ ,  $A_{prod}$  is a production asymmetry of  $D^{*+}$  mesons. To get  $\mathcal{A}_{CP}(K^+ K^-)$  from  $A_{CP}^{raw}$ ,  $A_{prod}$  and  $A_{det}$  are determined using Cabibbo favoured decays, as they have negligible CP-asymmetry. The determined  $\mathcal{A}_{CP}(K^+ K^-)$  is therefore,

$$\mathcal{A}_{CP}(K^+ K^-) = (6.8 \pm 5.4 \pm 1.6) \times 10^{-4},$$

where the first uncertainty is statistical and the second is systematic. This measurement is more precise than the current world average from HFLAV [5], illustrated in Fig. 3.

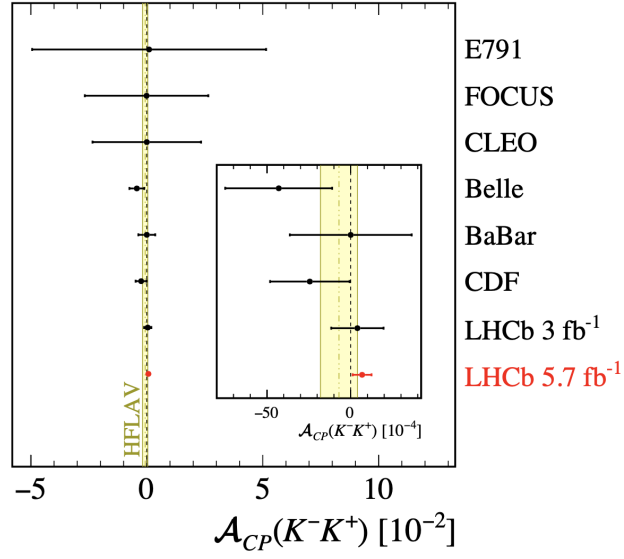


**Figure 3:** Experimental status of  $\mathcal{A}_{CP}(K^+K^-)$ . Highlighted in red is the LHCb result from [16].

Combining this result with the CP-asymmetry difference measured in [1] and previous LHCb measurement of  $\mathcal{A}_{CP}(K^+K^-)$  [19], the values for direct CP-asymmetries in  $D^0 \rightarrow K^+K^-$  decays and  $D^0 \rightarrow \pi^+\pi^-$  decays are determined:

$$a_{K^+K^-}^d = (7.7 \pm 5.7) \times 10^{-4},$$

$$a_{\pi^+\pi^-}^d = (23.2 \pm 6.1) \times 10^{-4}.$$

As can be seen from Fig. 4, the observed  $a_{\pi^+\pi^-}^d$  shows  $3.8\sigma$  deviation from CP-symmetry. This raises the need for a better understanding of this enhancement.

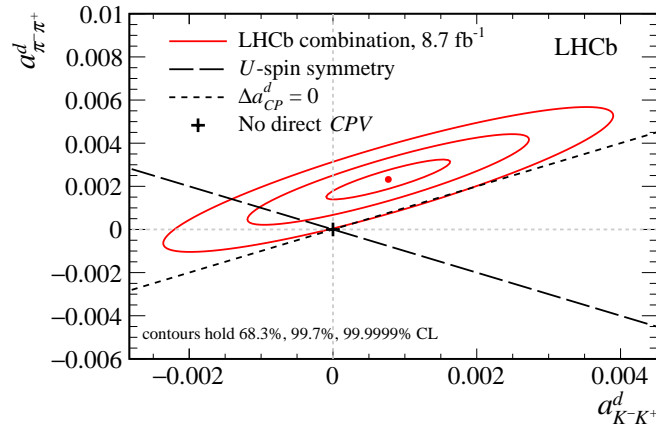


**Figure 4:** The combined direct CP asymmetry in  $D^0 \rightarrow K^+K^-$  decays and  $D^0 \rightarrow \pi^+\pi^-$  decays with LHCb data [16][19].

#### 4. CP violation in interference of mixing and decay

In  $B_{(s)}^0$  meson decays to a CP eigenstate, denoted by  $f$ , CP violation can originate from the interference between the mixing and the decay. The latter can be modelled by an effective Hamiltonian whose mass eigenstates are linear combinations of the two flavour eigenstates,  $p|B_s^0\rangle \pm q|\bar{B}_s^0\rangle$ , where  $p$  and  $q$  are complex parameters, normalised such that  $|p|^2 + |q|^2 = 1$ . The CP asymmetry as a function of decay time is given by

$$A_{CP}(t) = \frac{\Gamma_{\bar{B} \rightarrow f}(t) - \Gamma_{B \rightarrow f}(t)}{\Gamma_{\bar{B} \rightarrow f}(t) + \Gamma_{B \rightarrow f}(t)} = \frac{-C_f \cos(\Delta mt) + S_f \sin(\Delta mt)}{\cosh\left(\frac{\Delta\Gamma t}{2}\right) + A_f^{\Delta\Gamma} \sinh\left(\frac{\Delta\Gamma t}{2}\right)}, \quad (4)$$

where  $\Delta\Gamma$  and  $\Delta m$  are the widths and mass differences of the mass eigenstates of the  $B$  system,  $C_f$ ,  $S_f$  and  $A_f^{\Delta\Gamma}$  are defined as Eq. 5 and  $A_f$  ( $\bar{A}_f$ ) is the decay amplitude for the  $B_{(s)}^0$  ( $\bar{B}_{(s)}^0$ )  $\rightarrow f$  transition.

$$C_f = \frac{1 - |\lambda_f|^2}{1 + |\lambda_f|^2}, \quad S_f = \frac{2\Im\lambda_f}{1 + |\lambda_f|^2}, \quad A_f^{\Delta\Gamma} = \frac{2\Re\lambda_f}{1 + |\lambda_f|^2}, \quad \text{with } \lambda_f = \frac{q}{p} \frac{\bar{A}_f}{A_f}. \quad (5)$$

##### 4.1 CP-violation in $B^0 \rightarrow \psi K_S^0$ decays with $5.7 \text{ fb}^{-1}$

The updated analysis of the  $B^0 \rightarrow \psi K_S^0$  decay performed with the data set collected by the LHCb detector during the data-taking period from 2015 to 2018, where  $\psi$  represents either a  $J/\psi$  or a  $\psi(2S)$ , is presented in [20]. This particular decay mode is usually called the "golden channel" for measuring the  $\beta$  angle, as it is predominantly dominated by a tree-level  $b \rightarrow c\bar{c}s$  transition and exhibits a distinct experimental signature. The denominator of Eq. 5 is assumed to be unity since the measurement of the decay-width difference,  $\Delta\Gamma_d$ , is compatible with zero [5].

This analysis includes, for the first time, the following modes together  $B^0 \rightarrow J/\psi(\mu^+\mu^-)K_S^0$ ,  $B^0 \rightarrow J/\psi(e^+e^-)K_S^0$ ,  $B^0 \rightarrow \psi(2S)(\mu^+\mu^-)K_S^0$ , where the  $K_S^0$  is reconstructed from two charged pions tracks. To statistically subtract the background, the sPlot technique is employed [21]. The invariant mass distribution of the selected candidates of all the decay modes and reconstruction categories with the fit function and the background sources considered in the analysis is shown on the left plot of Fig. 5. The experimental resolution related to the reconstruction of the decay time is considered in the fit by convolving the probability density function (PDF) with three Gaussian functions centred at zero with widths defined as linear functions of the decay time error. The decay time efficiency is modelled using cubic splines [22]. The flavour of the  $B^0$  meson at production is inferred using the opposite-side (OS) taggers [23] and the same-side pion (SS $\pi$ ) and same-side proton (SSp) algorithms [24]. The estimated mistag probability,  $\eta$ , obtained by these algorithms is calibrated using flavour-specific decays [20]. The CP-violation parameters  $S$  and  $C$  are determined from a maximum-likelihood fit to the time-dependent decay rates of the  $B^0$  and  $\bar{B}^0$  decays. The decay time distribution of the signal candidates, as well as the CP fit projections for each of the signal modes, are shown on the right plot of Fig. 5. In Fig. 6, the observed  $B^0 - \bar{B}^0$  time-dependent asymmetry is shown for all the decay channels [20]. The CP violation parameters from

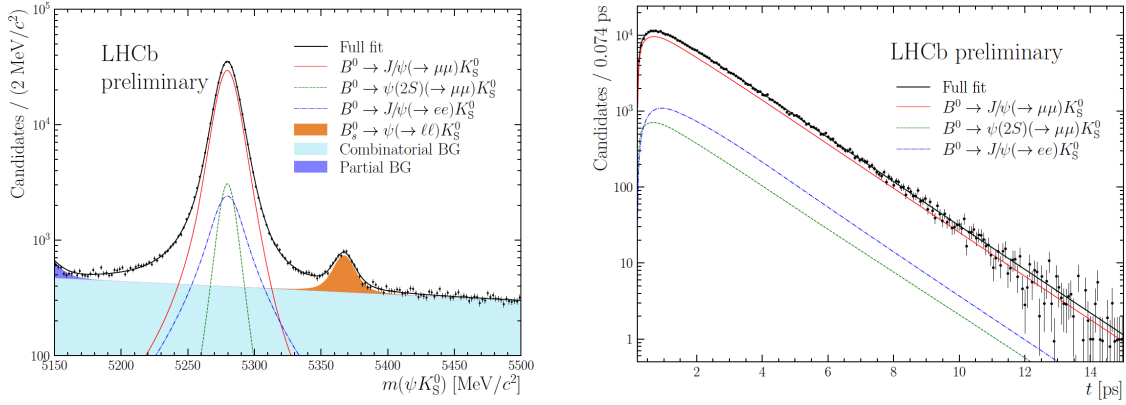


**Figure 5:** The invariant-mass distribution of the selected candidates is shown on the left figure (black points), as well as the three signal modes and the background sources considered in the extended likelihood fit. On the right plot, the decay time distribution of the signal is shown (black points), and the projections of the CP fit for the individual contributions of the three decay modes, and the total is superimposed.

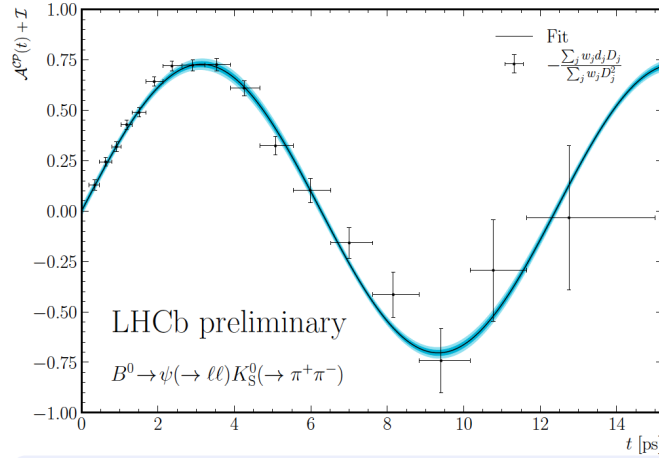


**Figure 6:**  $B^0 - \bar{B}^0$  decay time asymmetry weighted by the inverse of the Flavour tagging dilution (black points) and CP fit projections of the combined fit for the Run2 data set (black line). Dark and light blue regions correspond to  $1\sigma$  and  $2\sigma$  confidence interval of the statistical uncertainty of the fit. The small offset  $\mathcal{I}$  from 0 is due to production and flavour tagging asymmetries.

the simultaneous fit to the three decay channels are found to be [20]:

$$S_{\psi K_S^0}^{\text{Run2}} = 0.7158 \pm 0.0133 \text{ (stat.)} \pm 0.0078 \text{ (syst.)},$$

$$C_{\psi K_S^0}^{\text{Run2}} = 0.0120 \pm 0.0123 \text{ (stat.)} \pm 0.0029 \text{ (syst.)}.$$

The precision of this measurement is higher than the previous world average as determined by the HFLAV group [5] and is in agreement with the current average as evaluated by the CKMfitter group [6] and the UTfit group [25].

## 4.2 CP-violation in $B_s^0 \rightarrow J/\psi K^+ K^-$ decays with $5.7 \text{ fb}^{-1}$

In this section, the most recent update regarding the measurement of the time-dependent CP asymmetry in  $B_s^0 \rightarrow J/\psi(\mu^+\mu^-)K^+K^-$  decay is presented. The analysis utilizes the data collected by the LHCb detector during the data-taking period from 2015 to 2018. This decay mode, often referred to as the "golden channel" for the  $B_s^0 - \bar{B}_s^0$  system, is highly advantageous for precisely measuring all the significant parameters of the  $B_s^0$  meson. These parameters include the CP-violation phase  $\phi_s$  in  $b \rightarrow c\bar{c}s$  transitions ( $= 2\beta_S$  in SM neglecting higher order penguin contributions [3]), the difference in decay widths between the light and heavy mass eigenstates,  $\Delta\Gamma_s$ , the difference of the average  $B_s^0$  and  $B^0$  meson decay widths,  $\Gamma_s - \Gamma_d$ , the  $B_s^0$  mass difference  $\Delta m_s$  and the direct CP-violation parameter,  $|\lambda|$  [26].

To account for the pollution of the S-wave dominated by the  $f_0(980)$  resonance, the analysis is performed in six  $m(K^+K^-)$  bins in the vicinity of the  $\phi(1020)$  resonance. As in the previous analysis, the sPlot technique assigns a per-event weight that statistically subtracts the background contributions [21]. The measurement of  $\phi_s$  requires disentangling between the CP-even and CP-odd decay amplitude components, which implies an angular analysis. The experimental decay time resolution is accounted for by convolving the PDF with a Gaussian resolution function with the per-event decay time error as the width. The decay time efficiency is corrected using a data-driven method with  $B^0 \rightarrow J/\psi K^*(K^+\pi^-)$  as the control channel modelled with a cubic spline function [22]. The three-dimensional angular efficiency correction is introduced through normalization factors in the PDF and is determined from simulated signal events that are iteratively corrected to match real data kinematics. The flavour of the  $B_s^0$  meson at production is inferred using the opposite-side (OS) taggers [23] and the same-side kaon (SSK) algorithm [24]. Each decision gives an estimated mistag probability  $\eta$ , calibrated using flavour-specific decays. The results of the main physics parameters obtained from the simultaneous maximum likelihood fit are found to be [26]:

$$\begin{aligned}\phi_s [\text{rad}] &= -0.039 \pm 0.022 \pm 0.006, \\ |\lambda| &= 1.001 \pm 0.011 \pm 0.005, \\ \Gamma_s - \Gamma_d [\text{ps}^{-1}] &= -0.0056_{-0.0015}^{+0.0013} \pm 0.0014, \\ \Delta\Gamma_s [\text{ps}^{-1}] &= 0.0845 \pm 0.0044 \pm 0.0024, \\ \Delta m_s [\text{ps}^{-1}] &= 17.743 \pm 0.033 \pm 0.009,\end{aligned}$$

The background-subtracted data distributions and the fit projections are shown in Fig. 7. The measurements of  $\phi_s$ ,  $\Delta\Gamma_s$  and  $\Gamma_s - \Gamma_d$  are the most precise measurements to date and agree with SM expectations. No evidence of CP violation is found. Relaxing the assumption of same CP violation parameters for all the polarization states shows no evidence of any polarization dependence. The results are consistent with the previous measurements in  $B_s^0 \rightarrow J/\psi K^+ K^-$  [27, 28] performed by LHCb collaboration, as well as with previous measurements in this decay channel performed by ATLAS [29] and CMS [30] collaborations.

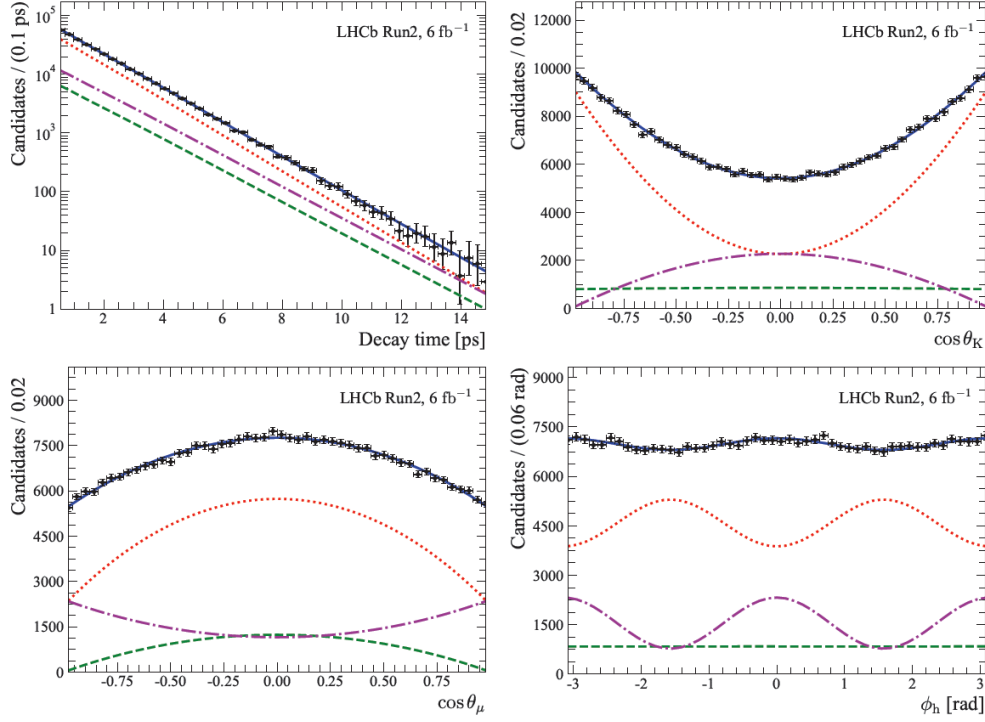


**Figure 7:** decay time and helicity angle distributions for background-subtracted  $B_s^0 \rightarrow J/\psi K^+ K^-$  decays (black points) and the one-dimensional projections of the total PDF (solid blue line), the CP-even contribution (dotted red), the CP-odd contribution (dash-dotted magenta) and the S-wave contribution (green).

#### 4.3 CP-violation in $B_s^0 \rightarrow \phi\phi$ decays with $5.7 \text{ fb}^{-1}$

The measurement of the CP violation parameters  $|\lambda|$  and  $\phi_s^{s\bar{s}s}$  in the penguin-mediated decay  $B_s^0 \rightarrow \phi\phi$  are also updated by the LHCb collaboration using data collected by the LHCb experiment during the Run2 data-taking (2015-2018) [31]. In contrast to the  $B_s^0 \rightarrow J/\psi KK$  decays, the interference phase which arises between the mixing and the decay through mixing in  $B_s^0 \rightarrow \phi\phi$  proceeds via a  $b \rightarrow s\bar{s}s$  transition. As a result, it is expected to be very close to zero due to a cancellation between the mixing and decay-weak phases. However, possible new physics contributions could arise and modify the CP-violation parameters,  $\phi_s^{s\bar{s}s}$  and  $|\lambda|$  [32].

The strategy employed in this analysis closely follows the approach described in Section 4.2, with the difference that the S-wave pollution is found to be negligible in this case. A signal weight is assigned to each candidate using the sPlot method from the fit to the invariant mass distribution of the selected  $B_s^0$  signal candidates [21]. The signal PDF includes the effects of angular and decay time efficiencies, decay time resolution and mistag dilution. The parameter  $\Delta m_s$ ,  $\Gamma_s$  and  $\Delta\Gamma_s$  are constrained using the most recent measurements by the LHCb collaboration [27, 33]. The CP violation parameters are found to be [31]:

$$\begin{aligned}\phi_s^{s\bar{s}s} [\text{rad}] &= -0.042 \pm 0.075 \pm 0.009, \\ |\lambda| &= 1.004 \pm 0.030 \pm 0.009.\end{aligned}$$

A polarization-dependent fit is performed where the parameters  $\phi_{s,i}$  and  $|\lambda|_i$ , being  $i$  each of the polarization states, can take different values. No significant difference between different polarization states is observed [31]. These results are combined with the LHCb previous measurement using the data-taking period from 2011 to 2012 [34], to obtain  $\phi_s^{\bar{s}s} = -0.074 \pm 0.069$  rad and  $|\lambda| = 1.009 \pm 0.030$ . This is the most precise measurement of time-dependent CP asymmetry in the decay  $B_s^0 \rightarrow \phi\phi$  and in any penguin-dominated  $B$  meson decay. The measurement is consistent with the SM expectation [31].

## 5. Prospects in LHC Run 3 and beyond

In the next years, LHC plans to collect more luminosity than ever. This will greatly benefit the CP-violation measurements. LHCb will collect  $50 \text{ fb}^{-1}$  of luminosity by the end of Run 4 (2032) and  $300 \text{ fb}^{-1}$  by the end of Run 6 (2041). Both CMS and ATLAS will have  $3 \text{ ab}^{-1}$  of data collected by the end of Run 6. Depending on the decay channel uncertainty on  $\gamma$  will be reduced to  $1^\circ - 4^\circ$  with  $50 \text{ fb}^{-1}$  LHCb dataset and to  $0.5^\circ - 2^\circ$  with  $300 \text{ fb}^{-1}$  LHCb dataset. Projections on parameters describing CP-violation in interference, like  $\sin 2\beta$  and  $\phi_s$ , depend greatly on the achievable flavour tagging power and decay time resolution. Assuming the expected Run 3 LHCb detector performance and trigger efficiency, the uncertainty on  $\sin 2\beta$  goes down to 0.006 with  $50 \text{ fb}^{-1}$ . With  $300 \text{ fb}^{-1}$  of integrated luminosity about 4 times improvement in uncertainty with respect to the current result [20] is expected. Projections on  $\phi_s$  uncertainty from  $B_s^0 \rightarrow J/\psi K^+ K^-$  decays are summarized in Fig. 8. LHCb future cases (Run 4 and Run 6) are shown assuming the current LHCb detector performance and improved trigger efficiency. For both CMS and ATLAS, the “best” scenario from [35] and [36] is shown.

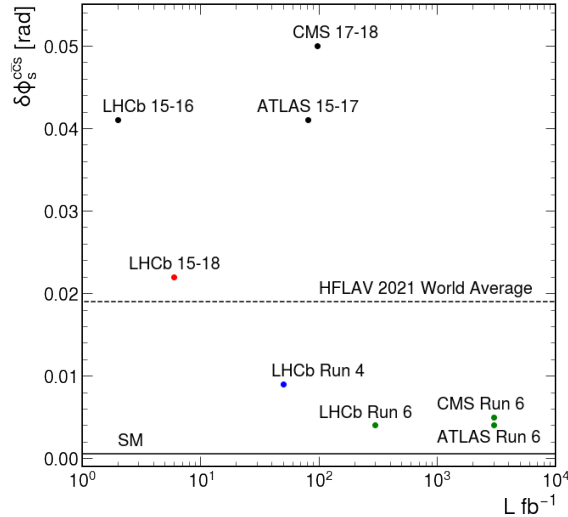


**Figure 8:** The projections on the statistical uncertainty of CP-violating phase  $\phi_s$  from  $B_s^0 \rightarrow J/\psi K^+ K^-$  decays. LHCb 15-16 is taken from [27], LHCb 15-18 from [26], CMS 17-18 from [30], ATLAS 15-17 from [29], LHCb Run 4 and Run 6 from [37], ATLAS Run 6 from [36] and CMS Run6 from [35]. HFLAV world average is from [5]. Standard Model value (SM) is taken from [6].

## References

- [1] LHCb collaboration, *Observation of CP Violation in Charm Decays*, *Phys. Rev. Lett.* **122** (2019) .
- [2] M. Kobayashi and T. Maskawa, *CP-Violation in the Renormalizable Theory of Weak Interaction*, *Prog. Theor. Phys.* **49** (1973) 652.
- [3] N. Cabibbo, *Unitary Symmetry and Leptonic Decays*, *Phys. Rev. Lett.* **10** (1963) 531.
- [4] J. Brod and J. Zupan, *The ultimate theoretical error on  $\gamma$  from  $B \rightarrow DK$  decays*, *JHEP* **2014** (2014) .
- [5] Y. Amhis et al., *Averages of b-hadron, c-hadron, and  $\tau$ -lepton properties as of 2018*, *Eur. Phys. J. C* **81** (2021) 226.
- [6] CKMFITTER collaboration, *CP violation and the CKM matrix: assessing the impact of the asymmetric b factories.*, *Eur. Phys. J. C* **41** (2005) .
- [7] LHCb collaboration, *Measurement of the CKM angle  $\gamma$  with  $B^\pm \rightarrow D[K^\mp \pi^\pm \pi^\pm \pi^\mp]h^\pm$  decays using a binned phase-space approach*, [2209.03692](#).
- [8] T. Evans, J. Libby, S. Malde and G. Wilkinson, *Improved sensitivity to the CKM phase  $\gamma$  through binning phase space in  $B^- \rightarrow DK^-$ ,  $D \rightarrow K^+ \pi^- \pi^- \pi^+$  decays*, *Phys. Lett. B* **802** (2020) 135188.
- [9] BESIII collaboration, *Measurement of the  $D \rightarrow K\pi^+\pi^+\pi^-$  and  $D \rightarrow K\pi^+\pi^0$  coherence factors and average strong-phase differences in quantum-correlated  $D\bar{D}$  decays*, *JHEP* **2021** (2021) .
- [10] LHCb collaboration, *First observation of  $D^0 - \bar{D}^0$  oscillations in  $D^0 \rightarrow K^+\pi^-\pi^+\pi^-$  decays and measurement of the associated coherence parameters*, *Phys. Rev. Lett.* **116** (2016) .
- [11] LHCb collaboration, *A study of CP violation in the decays  $B^\pm \rightarrow [K^+K^-\pi^+\pi^-]_D h^\pm$  ( $h = K, \pi$ ) and  $B^\pm \rightarrow [\pi^+\pi^-\pi^+\pi^-]_D h^\pm$* , [2301.10328](#).
- [12] LHCb collaboration, *Simultaneous determination of CKM angle  $\gamma$  and charm mixing parameters*, *JHEP* **2021** (2021) .
- [13] LHCb collaboration, *Measurement of the CKM angle  $\gamma$  with  $B^\pm \rightarrow D[K^\mp \pi^\pm \pi^\pm \pi^\mp]h^\pm$  decays using a binned phase-space approach*, [2209.03692](#).
- [14] LHCb collaboration, *Constraints on the CKM angle  $\gamma$  from  $B^\pm \rightarrow Dh^\pm$  decays using  $D \rightarrow h^\pm h'^\mp \pi^0$  final states*, *JHEP* **2022** (2022) .
- [15] LHCb collaboration, *Measurement of the charm mixing parameter  $y_{CP} - y_{CP}^{K\pi}$  using two-body  $D^0$  meson decays*, *Phys. Rev. D* **105** (2022) .
- [16] LHCb collaboration, *Measurement of the time-integrated CP asymmetry in  $D^0 \rightarrow K^- K^+$  decays*, [2209.03179](#).

- [17] LHCb collaboration, *Model-independent measurement of charm mixing parameters in  $\bar{B} \rightarrow D^0 (\rightarrow K_S^0 \pi^+ \pi^-) \mu^- \bar{\nu}_\mu X$  decays*, [2208.06512](#).
- [18] LHCb collaboration, *Simultaneous determination of the CKM angle  $\gamma$  and parameters related to mixing and CP violation in the charm sector*, Tech. Rep. , CERN, Geneva (2022).
- [19] LHCb collaboration, *Measurement of CP asymmetry in  $D^0 \rightarrow K^- K^+$  and  $D^0 \rightarrow \pi^- \pi^+$  decays*, *JHEP* **2014** (2014) .
- [20] LHCb collaboration, *Measurement of CP-violation in  $B^0 \rightarrow \psi (\rightarrow l^+ l^-) K_S^0 (\rightarrow \pi^+ \pi^-)$  decays*, [2309.09728](#).
- [21] M. Pivk and F.R. Le Diberder, *sPlot: a statistical tool to unfold data distributions*, *Nucl. Instrum. Meth.* **A555** (2005) 356 [[physics/0402083](#)].
- [22] LHCb COLLABORATION collaboration, *Precise determination of the  $B_s^0 - \bar{B}_s^0$  oscillation frequency*, *Nat. Phys.* **18** (2022) 1 [[2104.04421](#)].
- [23] LHCb COLLABORATION collaboration, *Opposite-side flavour tagging of B mesons at the LHCb experiment*, *Eur. Phys. J.* **C72** (2012) 2022 [[1202.4979](#)].
- [24] LHCb COLLABORATION collaboration, *A new algorithm for identifying the flavour of mesons at LHCb*, *JINST* **11** (2016) P05010 [[1602.07252](#)].
- [25] M. Bona et al., *The unitarity triangle fit in the standard model and hadronic parameters from lattice QCD: a reappraisal after the measurements of  $\Delta m_s$  and  $BR(B \rightarrow \tau \nu_\tau)$* , *JHEP* **2006** (2006) 081.
- [26] LHCb collaboration, *Improved measurement of CP violation parameters in  $B_s^0 \rightarrow J/\psi K^+ K^-$  decays in the vicinity of the  $\phi(1020)$  resonance*, [2308.01468](#).
- [27] LHCb collaboration, *Updated measurement of time-dependent CP-violating observables in  $B_s^0 \rightarrow J/\psi K^+ K^-$  decays*, *Eur. Phys. J.* **C 79** (2019) .
- [28] LHCb collaboration, *First measurement of the CP-violating phase in  $B_s^0 \rightarrow J/\psi (\rightarrow e^+ e^-) \phi$  decays*, *Eur. Phys. J.* **C 81** (2021) .
- [29] ATLAS collaboration, *Measurement of the CP-violating phase  $\phi_s$  in  $B_s^0 \rightarrow J/\psi \phi$  decays in ATLAS at 13 TeV*, *Eur. Phys. J.* **C 81** (2021) 342 [[2001.07115](#)].
- [30] CMS collaboration, *Measurement of the CP-violating phase  $\phi_s$  in the  $B_s^0 J/\psi \phi(1020) \rightarrow \mu^+ \mu^- K^+ K^-$  channel in proton-proton collisions at  $\sqrt{s} = 13$  TeV*, *Phys. Let. B* **816** (2021) 136188.
- [31] LHCb collaboration, *Precision measurement of CP violation in the penguin-mediated decay  $B_s^0 \rightarrow \phi \phi$* , [2304.06198](#).
- [32] T. Kapoor and E. Kou, *New physics search via CP observables in  $B_s^0 \rightarrow \phi \phi$  decays with left- and right-handed Chromomagnetic operators*, [2303.04494](#).

- [33] LHCb collaboration, *Precise determination of the  $B_s^0 - \bar{B}_s^0$  oscillation frequency*, *Nat. Phys.* **18** (2022) 1.
- [34] LHCb collaboration, *Measurement of CP violation in the  $B_s^0 \rightarrow \phi\phi$  decay and search for the  $B^0 \rightarrow \phi\phi$  decay*, *JHEP* **2019** (2019) .
- [35] CMS collaboration, *CP-violation studies at the HL-LHC with CMS using  $B_s^0$  decays to  $J/\psi\phi(1020)$* , Tech. Rep. , CERN, Geneva (2018).
- [36] ATLAS collaboration, *CP-violation measurement prospects in the  $B_s^0 \rightarrow J/\psi\phi$  channel with the upgraded ATLAS detector at the HL-LHC*, Tech. Rep. , CERN, Geneva (2018).
- [37] LHCb collaboration, *Physics case for an LHCb Upgrade II - Opportunities in flavour physics, and beyond, in the HL-LHC era*, [1808.08865](#).